A model for chemically-induced mechanical loading on MEMS

Fabien Amiot

A MODEL FOR CHEMICALLY-INDUCED MECHANICAL LOADING ON MEMS

F. AMIOT

Abstract. The development of full displacement field measurements as an alternative to the optical lever technique to measure the mechanical response for MEMS components in their environment calls for a modeling of chemically-induced mechanical fields (*i.e.,* stress, strain, and displacements). As these phenomena usually arise from species adsorption, adsorbate modification or surface reconstruction, they are surface-related by nature and thus require some dedicated mechanical modeling. The accompanying mechanical modeling proposed herein is intended to represent the chemical part of the system free energy and its dependence on the surface amount. It is solved in the cantilever case thanks to an asymptotic analysis, and an approached closed-form solution is obtained for the interfacial stress field. Finally, some conclusions regarding the transducer efficiency of cantilevers are drawn from the energy balance in the accompanying model, highlighting the role of surface functionalization parameters in micro-mechanical sensors engineering.

1. Introduction

The increasing interest in micro-electro-mechanical systems (MEMS) has raised the issue of several specific mechanical phenomena. Decreasing the size of mechanical objects down to the 1-100 micrometer range significantly enhances the surface-driven aspect of the mechanical behavior, so that these objects are used in a wide range of sensing applications [1]. In particular, the use of functionalized microcantilevers as environmental sensors has become very popular during the last decade. However, the basic understanding of the involved phenomena remains controversial because of numerous experimental parameters to control, and because of the lack of reliable spatially resolved mechanical information. For example, the basic understanding of the mechanisms involved in the mechanical effect induced by DNA hybridization at a cantilever surface remains an open issue [2, 3, 4, 5, 6], as well as the modeling of coupled phenomena such as electrocapillarity [7]. To overcome the latter difficulty, several authors [8, 9, 10, 11] have proposed the use of full displacement field measurements instead of the optical lever technique, to measure the microcantilever deformation. This has several advantages, depending on the way the displacement field is used, namely, averaging the displacement field across the cantilever allows one to increase the signal to noise ratio, if one is interested in a uniformly coated cantilever, and the selective readout of cantilevers functionalized in a heterogeneous manner can be achieved. Moreover, the use of full-field measurements leads to a significantly increased amount of information, which has to be compared to suitable mechanical models of surface phenomena. In particular, the widely used Stoney's equation [12] (which is obtained by assuming that the cantilever is subjected to a uniform mechanical effect) has to be enriched to describe the experimentally obtained displacement fields.

The goal of the present paper is to propose such a modeling, taking into account the finite size of the functionalized area to obtain a full displacement field instead of a mean curvature. The

Key words and phrases. Surface strains ; Variational formulation ; Surface coupling ; MEMS.

first section is devoted to derive such a mechanical modeling using thermodynamics arguments. Focusing on cantilever sensors, the chemical environment effect is represented by a mechanical layer, referred to as "the membrane" (bonded to the cantilever surface), whose thickness tends to zero. The solution for the interfacial shear-stress field is obtained by using the asymptotic expansion method [13, 14, 15] (Section 2). A general closed-form is proposed for the obtained shear-stress field, which depends on only three physical parameters. Last, a parametric study is carried out to provide some trends and perspectives to improve the efficiency of environmental sensors.

2. Mechanical modeling for chemically-actuated cantilevers

The accompanying mechanical modeling intended to represent the chemical part of the system free energy and its dependence on the surface amount is described in the first section.

2A. **Definition of the accompanying mechanical modeling.** Let us consider a representative interface element whose size is:

- small enough to satisfy the definiteness of partial derivatives involved in continuum mechanics;
- large enough to provide a representative description of the surface mechanical behavior.

These requirements are referred to as scale separation conditions in the following. For polycrystalline thin films, a representative element should then include at least 100 grains. Three phases are classically distinguished inside this interfacial element:

- a liquid phase, whose volume is V at pressure p. Several other state variables, denoted by the set $\{n_L^\alpha\}$, represent the amount of species α in the liquid phase, and thus describe its composition;
- the interphase, whose surface is S_i and composition is described by the set $\{n_S^\alpha\}$;
- the solid phase, whose surface is S_i, described by its stress field σ.

This system is assumed to be closed, in equilibrium with an external thermostat. The system is described by its Gibbs' free enthalpy $\mathcal{G}$. If the scale separation conditions are met, then the state variables set $\left\{T, p, \left\{\frac{n_L^\alpha}{V}\right\}, \left\{\frac{n_S^\alpha}{S_i}\right\}, \sigma\right\}$ describes the local interfacial state. In particular, the initial state corresponds to the sets $\left\{n_{L,0}^\alpha\right\}$ and $\left\{n_{S,0}^\alpha\right\}$. As one deals with a closed system, the conservation conditions lead to

$$dn_L^\alpha = -\beta^\alpha \tag{2-1}$$

$$dn_S^\alpha = \beta^\alpha \tag{2-2}$$

where β^α is the processed quantity for species α by the reaction

$$\alpha_{liquid} \xrightarrow{\beta^\alpha} \alpha_{interphase}$$

The system free enthalpy $\mathcal{G}$ reads

$$\mathcal{G} = \mathcal{G}_L + \mathcal{G}_S + \mathcal{G}_m = \mathcal{G}_c + \mathcal{G}_m \tag{2-3}$$

where $\mathcal{G}_L$ is the liquid phase contribution, $\mathcal{G}_S$ is the interphase one and $\mathcal{G}_m$ arises from the solid substrate. Both of the first two terms are formally merged into $\mathcal{G}_c$, which represents the chemical part in $\mathcal{G}$. Each free enthalpy contribution is expressed as a function of the state variables:

- the liquid phase is assumed to be an ideal solution, so that considering a unit volume, $\mathcal{G}_L$ reads

$$\mathcal{G}_L\left(p,T,\left\{\frac{n_L^\alpha}{V}\right\}\right)=\sum_\alpha \frac{n_L^\alpha}{V}\left[\mu_{L,0}^\alpha(p,T)+RT\log\left(\frac{n_L^\alpha}{V}\right)\right] \tag{2-4}$$

  where $\mu_{L,0}^\alpha(p,T)$ is the reference chemical potential at temperature T and pressure p for species α, R the molar gas constant.
- For the sake of generality, a general form for an elementary interphase portion is considered

$$\mathcal{G}_S\left(p,T,\left\{\frac{n_S^\alpha}{S_i}\right\}\right)=g\left(T,\left\{\frac{n_S^\alpha}{S_i}\right\}\right)+\sum_\alpha\left[\frac{n_S^\alpha}{S_i}\mu_{S,0}^\alpha(p,T)\right] \tag{2-5}$$

  where the function $g\left(T,\left\{\frac{n_S^\alpha}{S_i}\right\}\right)$ has to be chosen to represent the evolution of the adsorbate's free enthalpy as a function of the surface concentration. For instance, non-interacting adsorbate would lead to choose an expression g_{ni} for g similar to the one used in equation (2-4):

$$g_{ni}\left(T,\left\{\frac{n_S^\alpha}{S_i}\right\}\right)=RT\sum_\alpha\frac{n_S^\alpha}{S_i}\log\left(\frac{n_S^\alpha}{S_i}\right) \tag{2-6}$$

Setting $S_i=S_0+dS$, the chemical part of the overall free enthalpy reads

$$\begin{aligned}\mathcal{G}_c(S_i) \;=\; &\sum_\alpha\left[\frac{n_{L,0}^\alpha-\beta^\alpha}{V}\left[\mu_{L,0}^\alpha(p,T)+RT\log\left(\frac{n_{L,0}^\alpha-\beta^\alpha}{V}\right)\right]\right.\\ &\left.+\frac{n_{S,0}^\alpha+\beta^\alpha}{S_0+dS}\mu_{S,0}^\alpha(p,T)\right]+g\left(T,\left\{\frac{n_{S,0}^\alpha+\beta^\alpha}{S_0+dS}\right\}\right)\end{aligned} \tag{2-7}$$

The chemical contribution to the free enthalpy depends on the available surface amount. Considering small area variations

$$\begin{aligned}\mathcal{G}_c(S_i)\simeq\mathcal{G}_c(S_0)+\frac{1}{S_0}\sum_\alpha\left[-\left((n_{S,0}^\alpha+\beta^\alpha)\mu_{S,0}^\alpha(p,T)+\frac{\partial g}{\partial\left(\frac{n_S^\alpha}{S_i}\right)}\right)\frac{dS}{S_0}\right.\\ \left.+\left((n_{S,0}^\alpha+\beta^\alpha)\mu_{S,0}^\alpha(p,T)+\frac{\partial g}{\partial\frac{n_S^\alpha}{S_i}}+\frac{1}{2S_0}\frac{\partial^2 g}{\partial\left(\frac{n_S^\alpha}{S_i}\right)^2}\right)\left(\frac{dS}{S_0}\right)^2\right]+o\left(\frac{dS}{S_0}\right)^3\end{aligned} \tag{2-8}$$

Finally, both $\mathcal{G}_c$ and $\mathcal{G}_m$ depend on the available surface area. To include this shared dependence in the mechanical modeling of cantilevers, it is assumed that there is a virtual layer bonded to the surface under scrutiny, so that this surface and the virtual layer are constrained to deform together.

Moreover, it is considered that the virtual layer is subjected to a free strain ϵ_L. This local free strain value is identified by minimizing the free enthalpy assuming that no mechanical constrain is acting on the virtual layer, that is by minimizing the chemical term $\mathcal{G}_c$ with respect to the

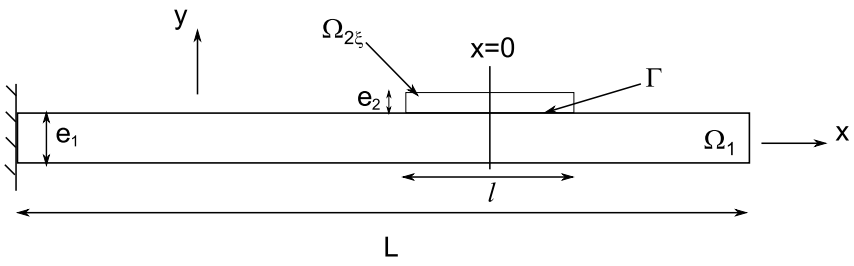

FIGURE 1. Schematic view of the accompanying mechanical model.

surface variation dS. Assuming that expansion (2-8) holds, ϵ_L satisfies

$$2 \times \epsilon_L \times \sum_\alpha \left[(n^\alpha_{S,0} + \beta^\alpha)\mu^\alpha_{S,0}(p,T) + \frac{\partial g}{\partial\left(\frac{n^\alpha_S}{S_i}\right)} + \frac{1}{2S_0}\frac{\partial^2 g}{\partial\left(\frac{n^\alpha_S}{S_i}\right)^2} \right] - \sum_\alpha \left[(n^\alpha_{S,0} + \beta^\alpha)\mu^\alpha_{S,0}(p,T) + \frac{\partial g}{\partial\left(\frac{n^\alpha_S}{S_i}\right)} \right] = 0 \tag{2-9}$$

If one prescribes, by any external mean, the virtual layer strain to be $\epsilon_L + \delta\epsilon$, its free enthalpy variation reads

$$\Delta\mathcal{G}_c = \left((n^\alpha_{S,0} + \beta^\alpha)\mu^\alpha_{S,0}(p,T) + \frac{\partial g}{\partial\left(\frac{n^\alpha_S}{S_i}\right)} + \frac{1}{2S_0}\frac{\partial^2 g}{\partial\left(\frac{n^\alpha_S}{S_i}\right)^2} \right) (\delta\epsilon)^2 \tag{2-10}$$

By analogy with the strain energy of a membrane, one is able to represent chemical effects by a bonded virtual membrane, whose thickness is denoted by e_v, whose Young's modulus E_v reads

$$E_v = \frac{2}{e_v S_0}\left((n^\alpha_{S,0} + \beta^\alpha)\mu^\alpha_{S,0}(p,T) + \frac{\partial g}{\partial\left(\frac{n^\alpha_S}{S_i}\right)} + \frac{1}{2S_0}\frac{\partial^2 g}{\partial\left(\frac{n^\alpha_S}{S_i}\right)^2} \right) \tag{2-11}$$

and whose free-strain satisfies (2-9). The equations (2-9) and (2-11) thus define, for a given membrane thickness e_v, an energetically equivalent mechanical modeling for the chemical effects. In addition to this energy equivalence, to account for the 2D nature of the phenomena under scrutiny, it is assumed that the virtual membrane thickness is small compared with that of the considered substrate. Consequently, the chemical effects are described by a virtual membrane whose thickness is small compared with the others, and which is constrained to deform together with the substrate surface, thus defining an accompanying mechanical modeling.

2B. **Initial problem.** The system is modeled as described in Fig. 1. The parameters related to the beam are denoted with the subscript $_1$, whereas those related to the thin layer (the membrane) are denoted with the subscript $_2$. The behavior of both the phases is assumed to be linear elastic. The beam obeys an Euler-Bernoulli kinematics, has a Young's modulus E_1, width b, length L and thickness e_1. This beam is then subjected to an axial free strain $\epsilon_{L1}(x)$. A thin membrane (whose Young's modulus is E_2, width b, length $l < L$ and thickness e_2) is constrained to deform together with beam 1 along the interface Γ when subjected to a free strain field $\epsilon_{L2}(x)$, $(-\frac{l}{2}) < x < (\frac{l}{2})$ (one sets $x = 0$ at the center of the membrane area). Denoting

by σ_1 the Cauchy stress tensor in cantilever 1, the interactions between the two beams are then represented by the scalar field $\tau(x)$ (shear-stress)

$$\sigma_1 \mathbf{y} = \tau(x)\mathbf{x} \tag{2-12}$$

where $\mathbf{x}$ denotes the unit vector in the cantilever's direction and $\mathbf{y}$ the outgoing normal to its upper surface. The equilibrium conditions read

$$\frac{dN_1}{dx} + \tau b = 0 \tag{2-13}$$

$$\frac{dM_1}{dx} - \tau b \frac{e_1}{2} = 0 \tag{2-14}$$

for cantilever 1 and

$$\frac{dN_2}{dx} - \tau b = 0 \tag{2-15}$$

for membrane 2, where N_i is the normal force in phase i and M_i the bending moment. It should be noted that the proposed modeling is expected to somehow fail to represent the mechanical effect induced by adsorbates subjected to strong in-plane interactions such as electrostatic interactions, since this would require to take the adsorbate's bending stiffness into account. The tension and bending problems are assumed to be decoupled for the cantilever 1, so that the constitutive law reads

$$M_1 = E_1 I_1 \frac{d^2 w}{dx^2} \tag{2-16}$$

where $E_1 I_1$ is the bending stiffness for cantilever 1 in the middle of the cross-section (homogeneous cantilever), $w(x)$ the out-of-plane displacement field of the assembly. At this point, it should be underlined that using a beam or membrane theory corresponds to specific forms for the Cauchy stress tensor and displacement (strain) fields inside the phases. According to St-Venant's principle, the computed fields will then be correctly predicted "far enough" from the loading application points, that is, in the described case, "far enough" from the interface. As a consequence, to describe the displacement at the interface, it is required to take into account the "local" contribution of the displacement field (*i.e.,* close to the interface) in addition to the long-range displacement field provided by beam or membrane theories. A closed-form solution to this local contribution is obtained using Kolossov-Muskhelishvili potentials [16] and expanding the shear-stress field onto a Legendre polynomial basis

$$\tau(x) = \sum_{k=0}^{\infty} \tau_k P_k \left(\frac{2x}{l} \right) \tag{2-17}$$

where $P_k(x)$ is Legendre polynomial of order k, and $\{\tau_k\}$ the projection of $\tau(x)$ onto the Legendre basis. The calculation of the in-plane displacement field $v(x)$ as the sum of the contributions $v_k(x)$ induced by the elementary shear-stress field $P_k\left(\frac{2x}{l}\right)$ is detailed in Appendix A, assuming the cantilever's material behavior to be isotropic. For the sake of simplicity, let us consider uniform free strain fields

$$\epsilon_{Li}(x) = \epsilon_{Li} \qquad i \in \{1, 2\} \tag{2-18}$$

The plane displacement on the interface for both the cantilever 1 and the membrane 2 read

$$u_1(x) - u_1\left(-\frac{l}{2}\right) = \epsilon_{L1} \times \left(x + \frac{l}{2}\right) + \int_{-\frac{l}{2}}^{x} \frac{N_1(\zeta)}{be_1E_1} d\zeta - \frac{e_1}{2}\int_{-\frac{l}{2}}^{x} \frac{d^2w}{d\zeta^2}(\zeta)d\zeta + \sum_{k=0}^{\infty} \tau_k v_k(x) \tag{2-19}$$

$$u_2(x) - u_2\left(-\frac{l}{2}\right) = \epsilon_{L2} \times \left(x + \frac{l}{2}\right) + \int_{-\frac{l}{2}}^{x} \frac{N_2(\zeta)}{be_2E_2} d\zeta + \frac{e_2}{2}\int_{-\frac{l}{2}}^{x} \frac{d^2w}{d\zeta^2}(\zeta)d\zeta \tag{2-20}$$

The kinematic compatibility condition at the interface reads

$$u_1(x) - u_1\left(-\frac{l}{2}\right) = u_2(x) - u_2\left(-\frac{l}{2}\right) \tag{2-21}$$

and has to be satisfied $\forall x, (-\frac{l}{2}) < x < (\frac{l}{2})$. Deriving equation (2-21) three times yields

$$-\left(\frac{1}{e_1E_1} + \frac{1}{e_2E_2} + \frac{be_1(e_1+e_2)}{4I_1E_1}\right)\frac{d\tau(x)}{dx} + \sum_{k=0}^{\infty} \tau_k v_k'''(x) = 0 \tag{2-22}$$

so that from equation (2-22), it is proved that neglecting the local contribution to the interface plane displacement leads one to prescribe $\frac{d\tau(x)}{dx} = 0$. Consequently, the equilibrium of the membrane would be satisfied if and only if the shear stress field vanishes. This result underlines the fact that it is necessary to describe the mechanical fields close to the interface in a much more detailed manner than classical phenomenological methods (see for instance [17]).

3. Variational formulation and asymptotic analysis

The aim of this section is to provide a suitable formulation of the problem to be solved to get the shear-stress field representing the environmental effect on the cantilever.

3A. **Complementary energy calculation for the initial problem.** The shear-stress field is found as the minimizer of the complementary energy of the overall structure. By assuming that there is no mechanical action on the membrane except the interaction with the beam, the set $\mathcal{V}$ of statically admissible shear-stress fields reads

$$\mathcal{V} = \left\{ \phi \in L^2\left(\left[-\frac{l}{2}, \frac{l}{2}\right]\right), \int_{-\frac{l}{2}}^{\frac{l}{2}} \phi(\zeta)d\zeta = 0 \right\} \tag{3-1}$$

Denoting by ξ the ratio between the thicknesses of the membrane and the beam

$$\xi = \frac{e_2}{e_1} \tag{3-2}$$

one defines the family of initial problems P_ξ as finding the shear-stress field $\tau_s(x)$ minimizing the complementary energy I_ξ

$$P_\xi : \left\{ \begin{array}{l} \tau_s(x) \in \mathcal{V} \\ I_\xi(\tau_s) \leq I_\xi(\phi) \qquad \forall \phi \in \mathcal{V} \end{array} \right. \tag{3-3}$$

with

$$I_\xi(\phi) = \Delta\Theta_1(\phi) + \Delta\Theta_{2,\xi}(\phi) \tag{3-4}$$

where $\Delta\Theta_1(\phi)$ and $\Delta\Theta_{2,\xi}(\phi)$ are the complementary energies for the cantilever and membrane, respectively, given by

$$\begin{aligned}\Delta\Theta_1(\phi) &= \frac{1}{2}\int_{\Omega_1}\sigma_{1,xx}(\phi)\varepsilon_{1,xx}(\phi)dV \\ &\quad -\int_\Gamma \phi(\zeta)\left(u_2(\zeta,z)-u_2\left(-\frac{l}{2},z\right)\right)dS + E_{d\tau}(\phi) \qquad (3\text{-}5)\\ \Delta\Theta_{2,\xi}(\phi) &= \frac{1}{2}\int_{\Omega_{2,\xi}}\sigma_{2,xx}(\phi)\varepsilon_{2,xx}(\phi)dV \\ &\quad -\int_\Gamma \phi(\zeta)\left(u_1(\zeta,z)-u_1\left(-\frac{l}{2},z\right)\right)dS \qquad (3\text{-}6)\end{aligned}$$

where $\varepsilon_{i,xx}$ is the linearized xx strain component in phase i and $E_{d\tau}(\phi)$ the strain energy in the localized deformation mode. It should be underlined that $I_\xi(\phi)$ (through the $\Delta\Theta_{2,\xi}$ term) is defined over a domain that depends on ξ. $I_\xi(\phi)$ is rewritten as

$$I_\xi(\phi) = a_\xi(\phi,\phi) - L(\phi) \qquad (3\text{-}7)$$

where the quadratic (resp. linear) forms a_ξ and L read

$$\begin{aligned}a_\xi(\phi,\phi) &= \left(\xi^{-1}\frac{1}{2E_2be_1}+\frac{1}{2E_1be_1}+\frac{2}{E_1be_1}\right)\int_{-\frac{l}{2}}^{\frac{l}{2}}N_1^2(\phi)dx \\ &\quad +\left(\xi^{-1}\frac{1}{e_1E_2}+\frac{1}{e_1E_1}+\frac{be_1^2(1+\xi)}{E_1I_1}\right)\int_{-\frac{l}{2}}^{\frac{l}{2}}\phi\int_{-\frac{l}{2}}^{x}N_1(\phi)d\zeta dx \\ &\quad +3E_{d\tau}(\phi) \qquad (3\text{-}8)\\ L(\phi) &= b(\epsilon_{L2}-\epsilon_{L1})\int_{-\frac{l}{2}}^{\frac{l}{2}}\phi\left(x+\frac{l}{2}\right)dx \qquad (3\text{-}9)\end{aligned}$$

The coercivity condition on the quadratic form a_ξ is lost when $\xi \to 0$. Consequently,

- from a practical point of view, the initial problem cannot be accurately solved by standard (*i.e.,* 3D) finite element formulations;
- from a theoretical point of view, formulation (3-3) falls out of the framework of the Lax-Milgram theorem, meaning that existence and uniqueness of its solution cannot be directly ensured.

Formulation (3-3) thus needs to be modified to get a reliable solution for the shear-stress field.

3B. **Scaled problem.** To transform P_ξ into a new problem defined on a fixed domain [14, 15] (*i.e.,* independent of ξ), one maps the domain

$$\Omega_{2,\xi} = \{\mathbf{x}_\Gamma + \xi y\mathbf{y}, y\in[0,e_1], \mathbf{x}_\Gamma\in\Gamma\} \qquad (3\text{-}10)$$

onto

$$\Omega_2 = \{\mathbf{x}_\Gamma + \tilde{y}\mathbf{y}, \tilde{y}\in[0,e_1], \mathbf{x}_\Gamma\in\Gamma\} \qquad (3\text{-}11)$$

The displacement fields in both phases, as well as the interfacial shear-stress field remain unscaled. It is then straightforward to check that if τ_s is a solution for (3-3), then $\tau_{s,\xi}$ is a solution for problem $\widehat{P}$

$$\widehat{P}:\left\{\begin{array}{l}\tau_{s,\xi}(x)\in\mathcal{V}\\ \widehat{I}_\xi(\tau_{s,\xi})\le\widehat{I}_\xi(\phi)\qquad \forall\phi\in\mathcal{V}\end{array}\right. \qquad (3\text{-}12)$$

where $\widehat{I_\xi}$ reads

$$\widehat{I_\xi}(\phi) = \widehat{a_\xi}(\phi,\phi) - L(\phi) \tag{3-13}$$

with the new quadratic form

$$\begin{aligned}\widehat{a_\xi}(\phi,\phi) &= \left(\xi\frac{1}{E_2be_1} + \frac{1}{E_1be_1} + \frac{4e_1^2}{E_1I_1}\right)\frac{1}{2}a_N(\phi,\phi) \\ &+ \left(\frac{\xi^{-1}}{e_1E_2} + \frac{1}{e_1E_1} + \frac{(1+\xi)be_1^2}{E_1I_1}\right)\frac{1}{2}a_d(\phi,\phi) + \frac{3b}{2}\times\frac{1}{2}a_\tau(\phi,\phi)\end{aligned} \tag{3-14}$$

where

$$a_N(\tau,\phi) = \int_{-\frac{l}{2}}^{\frac{l}{2}} N_1(\tau)N_1(\phi)dx \tag{3-15}$$

$$\frac{1}{2}a_d(\tau,\phi) = \frac{1}{2}\left\{\int_{-\frac{l}{2}}^{\frac{l}{2}}\tau\int_{-\frac{l}{2}}^{x} N_1(\phi)d\zeta dx + \int_{-\frac{l}{2}}^{\frac{l}{2}}\phi\int_{-\frac{l}{2}}^{x} N_1(\tau)d\zeta dx\right\} \tag{3-16}$$

$$\frac{1}{2}a_\tau(\tau,\phi) = \frac{1}{2}\left\{\int_{-\frac{l}{2}}^{\frac{l}{2}}\phi(x)v(\tau)(x)dx + \int_{-\frac{l}{2}}^{\frac{l}{2}}\tau(x)v(\phi)(x)dx\right\} \tag{3-17}$$

According to equation (2-11) it is assumed that the product ξE_2 tends to a finite value K_2 when ξ tends to 0

$$E_2 = K_2\xi^{-1} \tag{3-18}$$

so that this new quadratic form $\widehat{a_\xi}$ satisfies the Lax-Milgram conditions, and solving problem $\widehat{P}$ consists in finding the solution $\tau_{s,\xi}(x) \in \mathcal{V}$ for the linear system

$$\begin{aligned}\left(\xi^2\frac{1}{K_2be_1} + \frac{1}{E_1be_1} + \frac{4e_1^2}{E_1I_1}\right)a_N(\tau_{s,\xi},\phi) + \left(\frac{1}{e_1K_2} + \frac{1}{e_1E_1} + \frac{(1+\xi)be_1^2}{E_1I_1}\right)a_d(\tau_{s,\xi},\phi) \\ + \frac{3b}{2}a_\tau(\tau_{s,\xi},\phi) - L(\phi) = 0 \qquad \forall\phi\in\mathcal{V}\end{aligned} \tag{3-19}$$

The solution $\tau_{s,\xi}$ is then sought as a formal asymptotic expansion [13]

$$\tau_{s,\xi} = {}^0\tau + \xi\times{}^1\tau + \xi^2\times{}^2\tau + \dots \tag{3-20}$$

Putting equation (3-20) into the stationarity conditions (3-19) leads to a separate linear system for each ξ order. The leading term ${}^0\tau \in \mathcal{V}$ is found to satisfy

$$a_0({}^0\tau,\phi) - L(\phi) = 0 \qquad \forall\phi\in\mathcal{V} \tag{3-21}$$

with

$$\begin{aligned}a_0(\tau,\phi) &= \left(\frac{1}{E_1be_1} + \frac{4e_1^2}{E_1I_1}\right)a_N(\tau,\phi) \\ &+ \left(\frac{1}{e_1K_2} + \frac{1}{e_1E_1} + \frac{be_1^2}{E_1I_1}\right)a_d(\tau,\phi) + \frac{3b}{2}a_\tau(\tau,\phi)\end{aligned} \tag{3-22}$$

A finite dimension space $\mathcal{V}$ is chosen, described by the orthogonal basis of Legendre polynomials $P_n, n\in\{1,\dots N\}$, so that,

$${}^0\tau(x) = \sum_{k=1}^{N}{}^0\tau_k P_k\left(\frac{2x}{l}\right) \tag{3-23}$$

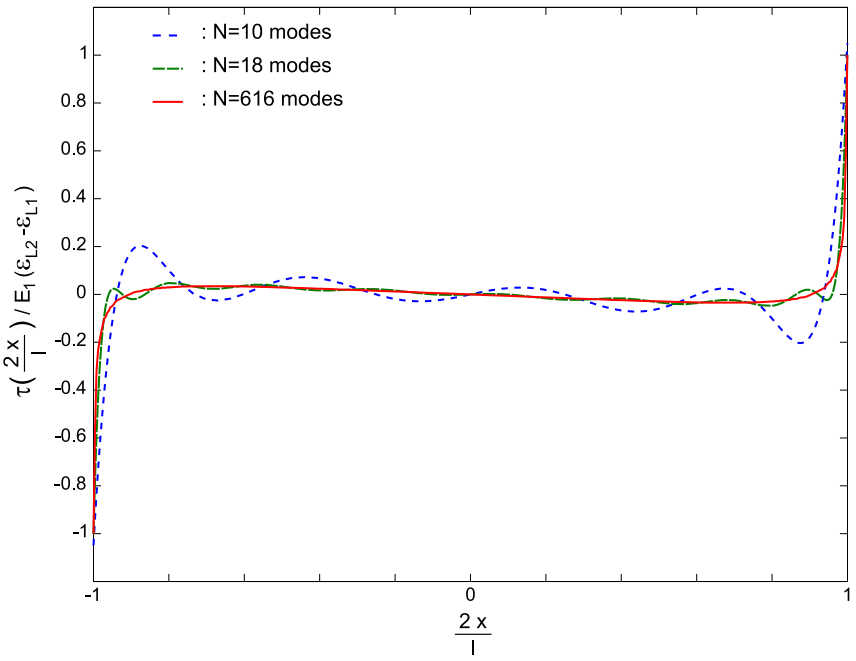

FIGURE 2. Convergence of the computed shear-stress field with the space dimension N.

System (3-21) then yields a square linear system, which is solved to provide the shear-stress field ${}^0\tau(x)$ along the interface Γ as its expansion (3-23).

4. Data reduction and parametric study

Even though the description of the shear stress field by its expansion with Legendre polynomials is natural from the mathematical point of view (see appendix A), this is of little practical interest. After demonstrating the convergence of the computed shear-stress field with the space dimension N, a closed-form solution for the interfacial stress field is provided, and from the above results some practical conclusions concerning the transducer efficiency are derived.

4A. **Convergence and data reduction.** By using the variational formulation obtained above, the (normalized) shear-stress field is calculated as a function of three physical parameters, namely,

- the geometrical parameter $s = \frac{l}{e_1}$;
- the modulus ratio $r = \frac{E_1}{K_2}$;
- the Poisson's ratio ν

Figure 2 shows the shear-stress field computed under plane strain conditions when $N = \{10, 18, 616\}$ and the following parameters $s = 0.1$, $r = 1$ and $\nu = 0.3$ are chosen. The reference solution is obtained with about 400-500 terms. All the even terms (*i.e.,* Legendre polynomials of even orders) vanish, since the solution is an odd function of the position. The shear-stress field is linear with the position at the center of the interval and drastically increases (in norm) close to the edges, but remains bounded. This reference shear-stress field, expressed as a series of Legendre's polynomials, is denoted τ_{ref} in the following.

To make these results useful, the shear stress field is modelled by using a closed-form solution $\tau\left(\frac{2x}{l}\right)$:

$$\frac{1}{E_1(\epsilon_{L2}-\epsilon_{L1})}\tau\left(\frac{2x}{l}\right) = T_t \tan\left(C\frac{\pi x}{l}\right) + T_l\frac{2x}{l} \tag{4-1}$$

where the constants C, T_t and T_l have to be identified from the computed shear-stress fields $\tau_{ref}(\frac{2x}{l})$. The reference shear-stress field has thus been computed in the following parameters range : $0.1 \leq \nu \leq 0.5$, $10^{-3} \leq r \leq 10^3$ and $0 \leq s \leq 1$. The local displacement contributions v_k have been obtained assuming the membrane's length to be small compared to the cantilever's thickness (see Appendix A). As the "local" contribution is significant over a depth which scales as l under the interphase, the upper bound for the s range is chosen to comply with the validity domain for the in-plane displacement field calculation, that is $s \leq 1$. The range for ν and r is supposed to cover most practical cases. An approached closed-form solution $\tau\left(\frac{2x}{l}\right)$ for the shear-stress field is obtained by minimizing

$$\chi^2 = \frac{\int(\tau(\frac{2x}{l}) - \tau_{ref}(\frac{2x}{l}))^2 dx}{\int \tau_{ref}(\frac{2x}{l})^2 dx} \tag{4-2}$$

over the set $\{C, T_t, T_l\}$. The identified values are recasted as

$$\begin{aligned} C &= (-1.47\times10^{-2}\nu^2 - 3.71\times10^{-3}\nu + 0.9957) \\ &\quad +10^{-4}\times(29.4\nu^2 + 3.87\nu + 4.92)t^{0.3217-6.23\times10^{-2}\nu} \qquad (4\text{-}3) \\ T_t &= (1.72\times10^{-1}\nu^2 - 4.73\times10^{-3}\nu + 5.5\times10^{-2}) \\ &\quad +10^{-3}\times(-45.3\nu^2 + 4.09\nu - 7.01)t^{0.313-5.47\times10^{-2}\nu-6.38\times10^{-2}\nu^2} \qquad (4\text{-}4) \\ T_l &= (-8.93\times10^{-1}\nu^2 - 3.36\times10^{-2}\nu - 3.61\times10^{-1}) \\ &\quad +10^{-2}\times(11.9\nu^2 + 0.182\nu + 1.41)t^{(4.52-1.71\nu)\times10^{-1}} \qquad (4\text{-}5) \end{aligned}$$

with

$$t = s(75 + 2r) \tag{4-6}$$

The maximum relative deviation $|\chi|$ between the reference solution τ_{ref} and the proposed closed form solution τ is found to be less than 7% over the entire parameters range, thereby proving the close agreement between the reference and closed-form solutions. For practical stress estimations, it is worth noting that all stresses, including the interfacial shear-stress, scale as the longitudinal stress for the 1D inclusion problem $|\epsilon_{L2}-\epsilon_{L1}|E_1$. From closed-form solution (4-1), the curvature field is obtained by using equations (2-14) and (2-16)

$$\frac{1}{E_1(\epsilon_{L2}-\epsilon_{L1})}\frac{d^2w}{dx^2} = -\frac{e_1 b}{2E_1 I_1}\left\{\frac{T_t l}{C\pi}\ln\left|\frac{\cos\left(\frac{C\pi x}{l}\right)}{\cos\left(\frac{C\pi}{2}\right)}\right| + T_l\left(\frac{l}{4} - \frac{x^2}{l}\right)\right\} \tag{4-7}$$

which is integrated using polylogarithm functions to provide the out-of plane displacement field. Considering a single functionalized area, this integration obviously yields the fact that the longer the distance between the membrane and the cantilever's edge, the greater the end-point displacement. It is worth noting that, similarly to the well-known shear-lag problem [19, 20, 21], the above described stress-field doesn't vanish near the membrane edges, since the whole interface is subjected to shear-stress. On the other hand, this stress field exhibits a rather different form than the one obtained with the shear-lag problem : the former diverges as $\tan(x)$ while the latter behaves as $\exp(x)$. This is thought to be the consequence of rather different interface conditions:

- the kinematic compatibility is ensured through a thin adhesion layer (typically a glue layer between two plies of a composite material) for the shear-lag problems ;

- no adhesion layer is considered here, but the kinematic compatibility at the interface is ensured considering the local elastic displacement field to enrich the beam kinematic description.

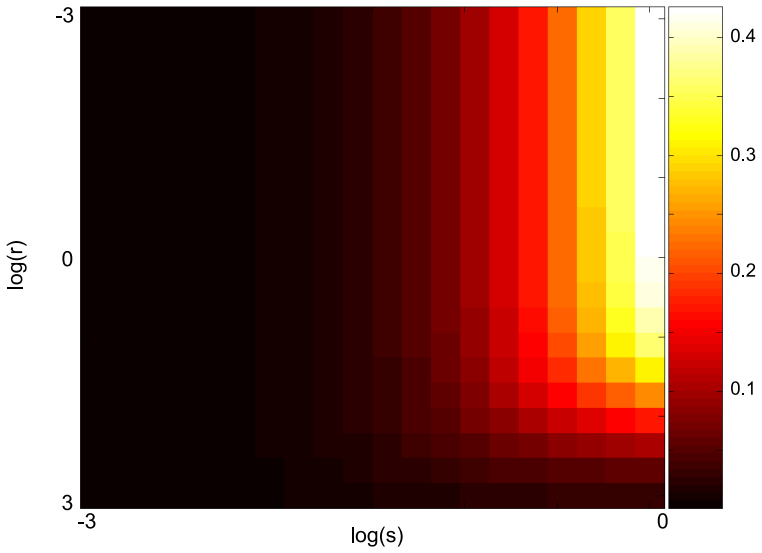

FIGURE 3. Overall transducer efficiency η as a function of the parameters r and s (log scales) when $\nu = 0.3$.

4B. **Transducer efficiency.** Moving back to the thermodynamic grounds of the modeling, and focusing on the sensing applications, the total energy in the accompanying model $\mathcal{E}_{tot}$ is decomposed as the following :

$$\mathcal{E}_{tot} = \mathcal{E}_{1,flex} + \mathcal{E}_{1,tens} + \mathcal{E}_{1,surf} + \mathcal{E}_2 \tag{4-8}$$

where

- $\mathcal{E}_{1,flex}$ is the strain energy located in the bending mode of the cantilever, so that it represents the useful part of the energy when the detection scheme relies on the cantilever bending ;
- $\mathcal{E}_{1,tens}$ is the strain energy located in the tension mode of the cantilever ;
- $\mathcal{E}_{1,surf}$ is the strain energy transferred to the "local" (surface) deformation mode of the cantilever ;
- $\mathcal{E}_2$ is the strain energy of the membrane, and thus represents, according to the equivalence principle which lead to the Equations (2-9), (2-10) and (2-11), the chemical energy stored in the system.

The sensing problem can then be expressed as converting the stored chemical energy $\mathcal{E}_2$ into some bending strain energy $\mathcal{E}_{1,flex}$. The transducer efficiency η is thus defined as

$$\eta = \frac{\mathcal{E}_{1,flex}}{\mathcal{E}_{tot}} \tag{4-9}$$

η is then the ratio of the energy used to produce the signal in most sensing applications [1] to the available energy. The ratio η is virtually independent of ν, and its change with the

parameters r and s is shown in Figure 3 when $\nu = 0.3$. Let us first consider that any typical length for the functionalized area is attainable for any considered cantilever's material using suitable functionalization techniques. This statement implies that any point in the (r, s) plane described in Figure 3 is achievable. The change of η with the parameter r is intuitive, namely, for a given K_2, decreasing $r = \frac{E_1}{K_2}$ is a way of improving the sensor efficiency, as was utilized with the development of polymeric cantilevers [22]. It should be underlined that if this trend is verified, the transducer efficiency does not vary significantly with r when $r \leq 1$, thus setting a limit to the transducer efficiency improvement one could achieve by reducing the cantilever's material stiffness. This optimal efficiency is then about 0.4, obtained when $r \to 0$ and $s \to 1$. The drastic efficiency loss when $r \gg 1$ is the result of the large amount of chemically "stored" (or blocked) energy in this range. The latter is monitored through the ratio ϱ, defined as

$$\varrho = \frac{\mathcal{E}_2}{\mathcal{E}_{tot}} \tag{4-10}$$

Figure 4 shows the ratio ϱ of the stored chemical energy (*i.e.,* the final strain energy in the

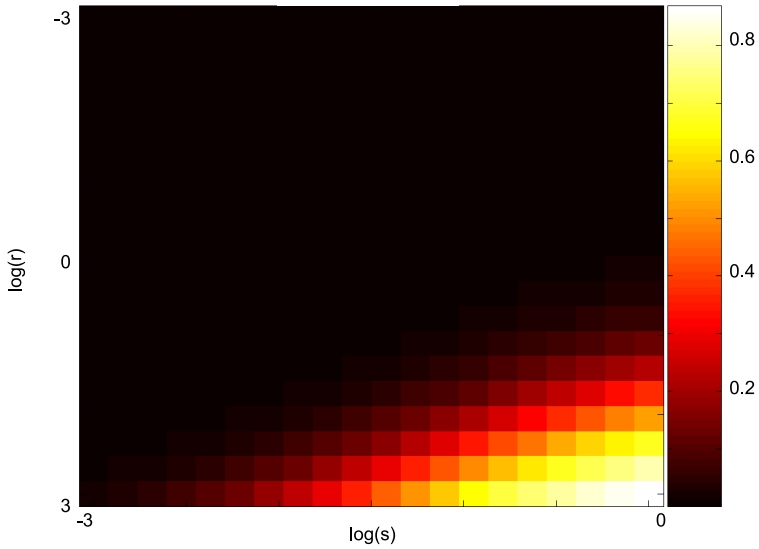

FIGURE 4. Ratio ϱ of the blocked chemical energy over the total system energy as a function of the parameters r and s (log scales) for $\nu = 0.3$.

membrane $\mathcal{E}_2$) over the total system energy as a function of the parameters r and s when $\nu = 0.3$. For instance, this ratio is found to be around 0.85 for $r = 10^3$ and $s = 1$, meaning that only 15% of the available chemical energy is used to produce a mechanical effect, and only part of this "mechanical" energy is used to bend the cantilever, the rest being mainly spent in the local deformation mode. This argument should be used carefully, especially if one is interested in non-invasive sensing applications. If the monitored chemical system is supposed to interact with some low concentration reagents, there is a balance between the transducer efficiency and the amount of energy taken from the chemical system to bend the cantilever to ensure the measurement's non-invasiveness, that is to ensure the energy used to bend the cantilever is small enough compared to the stored chemical energy.

The change of η with the size parameter s, described in Figure 3 is less intuitive. It should be noted that the cantilever's length (or the ratio of the membrane's length over the cantilever's one) is not involved at this stage. The possibility of converting more chemical energy into a mechanical one by extending the functionalized area is thus not considered here. For a given value of the membrane's size l, decreasing the cantilever's thickness e_1 is increasing the transducer efficiency. This results from the fact the surface deformation mode extends over a depth l under the surface (see Appendix A). The described coupling efficiency change is only related to the fact that the thinner the cantilever (i.e. the higher the s parameter), the more efficiently the strain energy located in the "local" (i.e. surface) deformation mode (which is not monitored so far) is converted into strain energy located into the cantilever bending mode (which is usually monitored using optical or piezoresistive read-out). This scaling effect is thus distinct from the lowering of the bending stiffness obtained by decreasing the cantilever's thickness. This raises comments regarding both the engineering and the basic understanding of the involved phenomena:

- In the previous discussion it was assumed that it is possible to move independently along both the axis of figures 3 and 4. From a practical point of view, this is false since chemical patterning techniques are substrate-dependent. Moreover, there is no experimental evidence that the K_2 value is not substrate dependent. Consequently, all the regions in Figures 3 and 4 are not attainable, and tailoring a cantilever based sensor is then balancing transducer efficiency and sensor invasiveness in the available parameters domain.
- The widely used alkanethiols adsorption on gold is known to follow a two-step adsorption process, namely a random adsorption process followed by a reorganization step [23]. The typical length describing the thiol-modified surface is then supposed to grow during the adsorption process. The transducer efficiency η dependance on the membrane's size may then play a key role in the inception of the observed mechanical effects, and the observed gap between the kinetics of the optical and the mechanical effects induced by this adsorption process [24].

Finally, both of these comments raise the need for the simultaneous experimental description of the functionalization pattern and the observed mechanical effect.

5. Conclusion

A thermodynamics-based modeling of chemically-induced mechanical loadings was described. The effect of the environment is described by an accompanying mechanical modeling representing the chemical part of the system free energy and its dependence on the surface amount. A dedicated variational formulation was proposed to solve this model for the surface stress, which is finally described by an approached closed-form expression depending on three parameters. The curvature field is also expressed as a closed-form solution, allowing for future comparisons with experimentally obtained fields. Finally, a parametric study was carried out, highlighting the need, for both the engineering and basic understanding point of view, to control the functionalization pattern.

Acknowledgement

The author would like to thank research professor F. Hild for the stimulating discussions from which this work originates.

Appendix A. In-plane displacement field calculation

The aim of this appendix is to compute the in-plane displacement field of the surface induced by a heterogeneous shear-stress field applied to the surface of a homogeneous half-space. To comply with the cantilever case (*i.e.,* a one-dimensional model), the calculation is restricted to the $(\mathbf{x},\mathbf{y})$ plane, by considering the elastic half-plane $y<0$. For the sake of simplicity, its behavior is described by its Young's modulus E and its Poisson's ratio ν. This half-plane is loaded along the line $y=0, -1<x<1$ by an elementary shear-stress field

$$\sigma_{xy}(x,0)\begin{cases} = P_k(x) & \text{if} \quad -1\leq x\leq 1 \\ = 0 & \text{if} \quad |x|>1 \end{cases}$$

where P_k is Legendre polynomial of order k. Moving to the complex plane and setting $z=x+iy$, the derivatives Φ and Y of the Kolossov-Muskhelishvili potentials [16] φ and Ψ read

$$\Phi_k(z) = \frac{1}{2\pi}\int_{-1}^{1}\frac{P_k(r)}{r-z}dr \tag{A-1}$$

$$Y_k(z) = -\frac{1}{\pi}\left\{\int_{-1}^{1}\frac{P_k(r)}{r-z}dr+\frac{z}{2}\int_{-1}^{1}\frac{P_k(r)}{(r-z)^2}dr\right\} \tag{A-2}$$

Using the properties of Legendre functions of first $P_k(z)$ and second kinds $Q_k(z)$ (see for instance [18]), and extending the definition of $Q_k(z)$ to the $y=0, -1<x<1$ segment by continuity from the $y<0$ side, one gets

$$\Phi_k(z) = -\frac{1}{\pi}Q_k(z) \tag{A-3}$$

$$Y_k(z) = -\frac{1}{\pi}\left\{-2Q_k(z)+\frac{z}{2}\left(-\frac{1}{1-z}-\frac{(-1)^k}{1+z} -2\sum_{l=0}^{k-2l-1\geq 0}(2k-4l-1)Q_{k-2l-1}(z)\right)\right\} \tag{A-4}$$

From [16], the complex displacement field reads

$$2\mu U = \kappa\varphi - z\overline{\varphi'} - \overline{\Psi} \tag{A-5}$$

with

$$\mu = \frac{E}{2(1+\nu)} \tag{A-6}$$

and κ is defined by

$$\kappa\begin{cases} = 3-4\nu & \text{for plane strain} \\ = \frac{3-\nu}{1+\nu} & \text{for plane stress} \end{cases}$$

The plane component of the strain fields is obtained using

$$\begin{aligned} 2\mu v_k^{'}(z) &= Re\left[2\mu\frac{dU}{dz}\right] \\ &= Re\left[(\kappa-1)\Phi_k(z)-z\overline{\Phi_k^{'}(z)}-\overline{Y_k(z)}\right] \end{aligned} \tag{A-7}$$

The strain field is found to extend to a depth of the order of l, so that this local solution should be used for systems where l is less than the substrate thickness ($l\leq e_1$). The in-plane

displacement field of the interface v_k is then obtained by setting $z \in [-1,1]$ and assuming $v_k(-1) = 0$

$$
\begin{aligned}
2\pi\mu v_1 &= -(1+\kappa)\left\{\frac{Q_2 - Q_0}{3} - \frac{P_0}{2}\right\} && \text{(A-8)}\\
2\pi\mu v_2 &= -(1+\kappa)\left\{\frac{Q_3 - Q_1}{5} + \frac{P_0}{6}\right\} && \text{(A-9)}\\
2\pi\mu v_3 &= -(1+\kappa)\left\{\frac{Q_4 - Q_2}{7}\right\} + P_1 + (13+\kappa)\frac{P_0}{12} && \text{(A-10)}\\
2\pi\mu v_4 &= -(1+\kappa)\left\{\frac{Q_5 - Q_3}{9} + \frac{P_0}{20}\right\} && \text{(A-11)}\\
2\pi\mu v_{2p+1} &= -(1+\kappa)\left\{\frac{Q_{2p+2} - Q_{2p}}{4p+3}\right\} - \frac{Q_2 - Q_0}{3}\\
&\quad + \sum_{k=1}^{p} \theta_{k,p} P_{2(p-k)+1} + \tilde{\theta}_p P_0 \qquad \text{if } p > 1 && \text{(A-12)}\\
2\pi\mu v_{2p} &= -(1+\kappa)\left\{\frac{Q_{2p+1} - Q_{2p-1}}{4p+1}\right\} + \sum_{k=1}^{p} \lambda_{k,p} P_{2(p-k)}\\
&\quad \text{if } p > 2 && \text{(A-13)}
\end{aligned}
$$

where

$$
\begin{aligned}
\theta_{1,p} &= \frac{d_{1,p}}{4p-3} && \text{(A-14)}\\
\theta_{p,p} &= -\frac{d_{p-1,p}}{5} + \frac{1}{p+1} + b_{p,p} - \sum_{l=0}^{p-1} \frac{4(p-l)+1}{2(p-l)(2(p-l)+1)} && \text{(A-15)}\\
\theta_{k,p} &= \frac{d_{k,p}}{4(p-k)+1} - \frac{d_{k-1,p}}{4(p-k)+5} \qquad \text{if } 1 < k < p && \text{(A-16)}\\
\tilde{\theta}_p &= \frac{1+\kappa}{(2p+1)(2p+2)} + \frac{1}{2} + \frac{1}{p+1} + b_{p,p}\\
&\quad - \sum_{l=0}^{p-1} \frac{4(p-l)+1}{2(p-l)(2(p-l)+1)} && \text{(A-17)}\\
\lambda_{1,p} &= \frac{c_{1,p}}{4p-5} && \text{(A-18)}\\
\lambda_{p,p} &= -\frac{1+\kappa}{2p(2p+1)} - \frac{c_{p-1,p}}{3} && \text{(A-19)}\\
\lambda_{k,p} &= \frac{c_{k,p}}{4(p-k)-1} - \frac{c_{k-1,p}}{4(p-k)+3} \qquad \text{if } 1 < k < p && \text{(A-20)}
\end{aligned}
$$

with the constants

$$a_{r,p} = \sum_{k=0}^{r-1} \left\{ \frac{(4(p-k)-3)\,(4(p-r)-1)}{(2(r-k)-1)\,(2p-r-k-1)} - \frac{(4(p-k)-1)\,(4(p-r)-1)}{(2k+1)(2p-k)} \right\} \tag{A-21}$$

$$b_{r,p} = \sum_{k=0}^{r-1} \left\{ \frac{(4(p-k)-1)\,(4(p-r)+1)}{(2(r-k)-1)\,(2p-r-k)} - \frac{(4(p-k)+1)\,(4(p-r)+1)}{(2k+1)(2p+1-k)} \right\} \tag{A-22}$$

$$c_{r,p} = \frac{4(p-r)+1}{2p-r} + a_{r,p} - \frac{4(p-r)-1}{2(p-r)} - \sum_{k=1}^{r} \frac{(4(p-k)+3)\,(4(p-r)-1)}{2\,(2(p-k)+1)\,(p-k+1)} \tag{A-23}$$

$$d_{r,p} = \frac{4(p-r)+1}{2p+1-r} + b_{r,p} - \frac{4(p-r)+1}{2(p-r)+1} - \sum_{k=0}^{r-1} \frac{(4(p-k)+1)\,(4(p-r)+1)}{2\,(2(p-k)+1)\,(p-k)} \tag{A-24}$$

References

[1] Lavrik NV, Sepaniak MJ and Datskos PG 2004 *Review of Scientific Instruments* **75** 2229-2253
[2] Fritz J, Baller MK, Lang H P, Rothuizen H, Vettiger P, Meyer E, Gntherodt H, Gerber C and Gimzewski JK 2000 *Science* **288** 316-318
[3] Wu G, Ji H, Hansen K, Thundat T, Datar R, Cote R, Hagan MF, Chakraborty AK and Majumdar A 2001 *PNAS* **98** 1560-1564
[4] Hansen KM, Ji HF, Wu G, Datar R, Cote R, Majumdar A and Thundat T 2001 *Anal. Chem.* **73** 1567-1571
[5] McKendry R, Zhang J, Arntz Y, Strunz T, Hegner M, Lang HP, Baller MK, Certa U, Meyer E, Güntherodt H and Gerber C 2002 *PNAS* **99** 9783-9788
[6] Hagan FH, Majumdar A and Chakraborty AK 2002 *J. Phys. Chem. B* **106** 10163-10173
[7] Marichev VA 2005 *Surface Science Reports* **56** 277-324
[8] Helm M, Servant JJ, Saurenbach F and Berger R 2005 *Appl. Phys. Lett.* **87** 064101
[9] Mertens J, Álavarez M and Tamayo J 2005 *Appl. Phys. Lett.* **87** 234102
[10] Amiot F., Roger J. P. and Boccara A. C. 2003 *Advanced Biomedical and Clinical Diagnostic Systems* (SPIE) p. 183-8. See also : Amiot F., Hild F. and Roger J. P. 2006 *Int. J. SolidsStruct.* **44** 2863-2887
[11] Amiot F and Roger JP 2006 *Appl. Optics* **45** 7800-7810
[12] Stoney G 1909 *Proc. Roy. Soc. London Ser A* **82** 172
[13] Lions J-L 1973 *Perturbations singulières dans les problèmes aux limites et en contrôle optimal* (Berlin: Springer-Verlag)
[14] Klarbring A 1991 *Int. J. Eng. Sci.* **29** 493-512
[15] Geymonat G and Krasucki F 1997 *C. R. Acad Sci. Paris* **325** 307-314
[16] Muskhelishvili N. I. 1953 *Some basic problems of the mathematical theory of elasticity* (Grönigen (Holland): P. Noordholl Ltd)
[17] Cammarata R. C. 1994 *Progress in surface science* **46** 1-38
[18] Gradstein I. S. and Ryzhik I. M. 1980 *Tables of Integrals, Sums, Series and Products* (New York: Academic Press)
[19] Volkersen O. 1938 *Luftfahrtforschung* **15** 41-47
[20] Cox H. L. 1952 *Br. J. Appl. Phys.* **3** 72-79

[21] Lemaitre J., Sherman D. and Leckie F. A. 1992 *Eur. J. Mech. A/Solids* **11** 289-304
[22] Johansson A., Calleja M., Rasmussen P. A. and Boisen A. 2005 *Sensors and Actuators A* **123-124** 111-115
[23] Damos F. S., Luz R. C. S. and Kubota L. T. 2005 *Langmuir* **21** 602-609
[24] Godin M., Laroche O., Tabard-Cossa V., Beaulieu L. Y., Grtter P. and Williams P. J. 2003 *Review of Scientific Instruments* **74** 4902-4907

MIC - DTU, Ørsted Plads, Bygning 345 Ø, DK-2800 Lyngby, Denmark
E-mail address: fabien.amiot@mic.dtu.dk